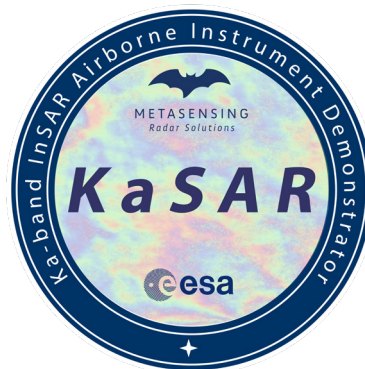


Ka-band InSAR Airborne Instrument Demonstrator (KaSAR)

Executive Summary Report

[D - 18]



Document Reference Code : D-18_MS-ESA-KAS-EXR-010

Date : 14/09/2022

	Name	Company
Prepared by	Simone Placidi	MetaSensing
	Karlus Macedo	MetaSensing
	Thiago Luiz	MetaSensing
	Adriano Meta	MetaSensing
Checked by	Adriano Meta	MetaSensing
Released by	Simone Placidi	MetaSensing

MetaSensing BV
Huygensstraat 44
2201 DK Noordwijk, The Netherlands
Tel.: +31 71 751 5960
Email: info@metasensing.com

[This page is intentionally left almost blank]

Document Information

Contract details	
Number:	4000116872/16/NL/FE
Issuer:	ESA – ESTEC
Contract Officer	Franziska Erkelens
Technical Officer	Ishuwa Sikaneta

Distribution List

Sent to	Affiliation	Date	Format
Ishuwa Sikaneta	ESA	16/09/2022	PDF

Document Change Log

Issue	Change description	Date	Author
1.0	Initial release	16/09/2022	



Table of Contents

1	The KaSAR project.....	8
1.1	Introduction	8
1.2	Instrument specifications	10
1.3	The functional verification campaigns	12
1.4	Conclusions	18

Index of Figures

Figure 1: MetaSensing's Piper PA-31 with the belly pod hosting the KaSAR instrument.....	8
Figure 2: Logical block diagram of the system.....	9
Figure 3: KaSAR instrument installed on Piper PA031	10
Figure 4: SAR image generated by the KaSAR Processor from data acquired by KaSAR	12
Figure 5: Piper PA31 aircraft modified with the belly pod for KaSAR	12
Figure 6: Position of the corner reflectors (yellow pins) and the track of the flight (red line)	13
Figure 7: SAR image with swath around 1750 m	13
Figure 9: NESZ estimation of -25dB.....	14
Figure 8: Full-pol KaSAR intensity images [dB] (20220504T163000) from top to bottom: RGB composite ((HH is red, VV is blue and HV is green) and zoomed-in in the corner reflector area.	14
Figure 10: Retrieved Interferograms: XTI above and ATI below	15
Figure 11: Coherence map for the XTI above case	16
Figure 12: Digital Elevation Model retrieved from the above interferograms	16
Figure 13: Comparison of heigh retrieval for the Corner Reflectors. (left - SAR image, right - DSM).....	16
Figure 14: Coherence map for the ATI above case with no spatial decorrelation over forest	17
Figure 15: ATI phases of the corners for the inter-channel phase accuracy calculation over time.....	17
Figure 16: Velocity map over intensity image.....	18

Acronyms and Abbreviations

ACS	Antenna Coordinate System
AT	Along Track
ATI	Along-Track Interferometry
BCS	Body Coordinate System
BPA	Back-Projection Algorithm
CTP	Conventional Terrestrial Pole
DC/DC	Direct Current/Direct Current
ECEF	Earth-Centred, Earth-Fixed
ECS	Extended Chirp Scaling
EOK	Extended Omega-K
FFT	Fast Fourier Transform
FMCW	Frequency-Modulated Continuous Wave
GCP	Ground Control Points
GPU	Graphics Processing Unit
IFFT	Inverse Fast Fourier Transform
LOS	Line of Sight
MOCO	Motion Compensation
NCS	Nadir Coordinate System
NED	North-East-Down
NRCS	Normalized Radar Cross-Section
PRF	Pulse Repetition Frequency
RDA	Range-Doppler Algorithm
RDM	Reflectivity Displacement Method
RX	Receive
RVP	Residual Video Phase
SLC	Single-Look Complex
TRS	Terrestrial Reference System
TX	Transmit
XT	Cross Track
XTI	Cross-Track Interferometry
WGS84	World Geodetic System 1984

Abstract

This document is the Executive Summary Report for the KaSAR development project under ESA-ESTEC contract number 4000116872/16/NL/FE.

Keywords

Synthetic Aperture Radar, Airborne Demonstrator, Interface Control Document, Interferometry, Ka-band, aircraft, airworthiness certification.

1 The KaSAR project

1.1 Introduction

The Ka-band frequency is receiving significant attention from various areas, especially for spaceborne remote sensing for Earth Observation applications. For several years, interest in the 35GHz frequency band has been growing, and the advantages and disadvantages for SAR systems are being investigated. The 35GHz band has already been used for certain applications, for example telecommunication from satellites as well as cloud and precipitation observations from the ground. However, it has so far not been used for Earth Observation from space.



Figure 1: MetaSensing's Piper PA-31 with the belly pod hosting the KaSAR instrument

The KaSAR project deals with the development of a multi-channel airborne SAR sensor at Ka-band with single-pass along-track (ATI) and across-track (XTI) interferometry with adjustable baselines, as well as polarimetry. The airborne segment is complemented with an offline interferometric SAR processor based on Global Back Projection algorithm running on parallel Graphics Processing Units (GPU). Additionally, the instrument, with its own airworthiness certification, is equipped with a camera for high-resolution optical images of the observed area to support data validation.

The selected aircraft carrier is MetaSensing's Piper PA-31, capable to host the KaSAR sensor for the data acquisition campaign in a dedicated airworthiness-certified belly pod radome.

The main development objective of the KaSAR instrument is to mimic and emulate a satellite

instrument, keeping in mind observation parameters which can be scaled to a potential satellite mission in future Earth Explorer programs. The system will be used to exploit the advantages of mm-wavelength technology for Earth Observation in different applications.

The four main items of the KaSAR project are as follow: the KaSAR airborne instrument, the ground SAR processor, the aircraft and instrument airworthiness certification, and the system functional verification campaign.

The KaSAR system can be depicted as in the block diagram shown in Figure 2.

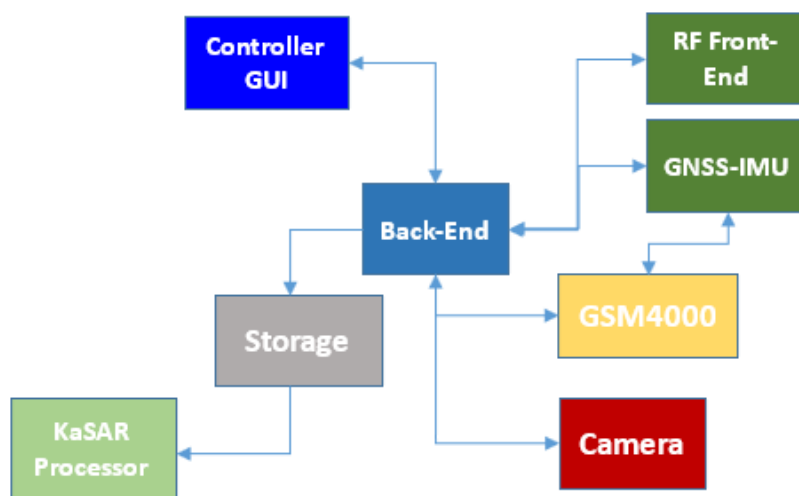


Figure 2: Logical block diagram of the system

The control GUI, installed on the operator computer, is connected to the radar firmware through TCP/IP protocols. All radar sub-systems and modules are connected to a computer in the digital back-end where the firmware developed by MetaSensing controls them all in synergy. Acquired data are stored in an array of SSHD set in RAID configuration to increase data rate and storage. The radar raw data together with the auxiliary data (calibration data, navigation data, devices logs, system health status logs) can be then ingested in the off-line KaSAR Processor for executing the SAR processing steps.



Figure 3: KaSAR instrument installed on Piper PA031

1.2 Instrument specifications

The KaSAR instrument features multiple transmit and receive channels that allow for baseline configurations capable of simultaneously acquiring multi-baseline single-pass along- and cross-track interferometry (ATI and XTI). These baselines are adjustable to ensure maximum configuration flexibility. The radar is based on frequency-modulated continuous-wave (FMCW) technology, with a bandwidth of 500 MHz centered at 35.75 GHz. The bandwidth has been selected to ensure a ground resolution better than 1 m over the swath, and it is adjustable to increase the instrument sensitivity. The sensor is composed of two 10 W independent transmitters, operating in toggled mode, and eight simultaneous receivers. Fully polarimetric configurations and ping-pong operation are possible (see Table 1 and Table 2 for the full specifications). The digital back end is mounted inside the aircraft cabin in a 19" rack. The instrument features a 3-axis stabilizer for accurate motion compensation and

steady antenna pointing, and it is equipped with a military graded IMU. A feedback loop between the stabilizer and the IMU has been implemented to improve the antenna pointing accuracy and ensure the uniformity of the desired baselines during the imaging time. The radar front-end (RF module and slotted waveguide antennas) are installed in a pod under the belly of the aircraft to minimize the losses. A military graded IMU is also installed in the pod near the antenna to track their position and attitude with high accuracy. The pod has been developed ad-hoc for the KaSAR instrument. The materials of the sandwich-A type radome and shape of the pod have been devised to minimize the insertion loss and to ensure phase uniformity of the different beams illuminating through the radome. In the RF module, an internal calibration is implemented to ensure very high phase and radiometric accuracies.

Table 1: KaSAR instrument hardware specifications.

Property	Value
Operating frequency	35.75 GHz
Modulation	FMCW
Bandwidth	500 MHz (adjustable)
Transmit power	10W
Number Tx channels	2 (toggled)
Number Rx channels	8 (simultaneous)
Data storage	8 TB
Antenna size (az x el)	0.1m x 0.05m
Antenna gain	22.3 dBi
Beamwidth (az x el)	4.5° x 35°
Cross-polar	< -27dB
Sidelobe level	< -15dB
Polarization	Dual linear (H & V)

Table 2: KaSAR instrument operational characteristics.

Property	Value
Height of operation	500m < h < 3000m
Incidence angles	20° - 50°
Operational modes	Mono-pol V, mono-pol H, full-pol V&H, ping-pong, dual-view L/R
Adjustable Baselines (RX antenna distance)	0.1m < ATB < 0.5m 0.1m < XTB < 0.4m
NESZ	<-20dB
Swath width	> 1km (resolution dependent)
Ground resolution	< 1m x 1m (SLC)
Inter-channel phase accuracy	< 1° RMS
Vertical accuracy (from the data)	~10cm flat areas (high coherence) ~50cm forested areas
Spaceborne reference scenario	400-800 km orbit height, 7 km/s speed, 16 km swath (NESZ < -16dB)



Figure 4: SAR image generated by the KaSAR Processor from data acquired by KaSAR



Figure 5: Piper PA31 aircraft modified with the belly pod for KaSAR

1.3 The functional verification campaigns

The final activity of the project is to perform a functional verification campaign to test the complete KaSAR chain from the instrument collecting the data to the generation of the SAR images, interferograms and coherence maps which can be used for further processing such as retrieval of velocities or digital elevation models.

The data acquisitions were performed with the objective of end-to-end testing the KaSAR hardware, including the radome, control software and processing software.

To verify the complete functionality of the KaSAR instrument the acquired raw data are processed with the KASAR processor, implementing therefore a complete end-to-end system verification.

The data are processed up to SLC level with 1x1 m resolution and 1km ground swath. With the packager module of the KaSAR processor, the intensity images and interferograms are generated and

visualised. A total of 4 tracks have been selected to verify the KaSAR instrument. These 4 tracks cover all possible modes of operation of the instrument, i.e monopoles (Single-polarimetric), ping-pong and full polarimetric mode in both ATI and XTI.

Corner reflectors were also positioned around the scene with their location logged in the files. Position of the corner reflectors, numbered with the heading.



Figure 6: Position of the corner reflectors (yellow pins) and the track of the flight (red line)

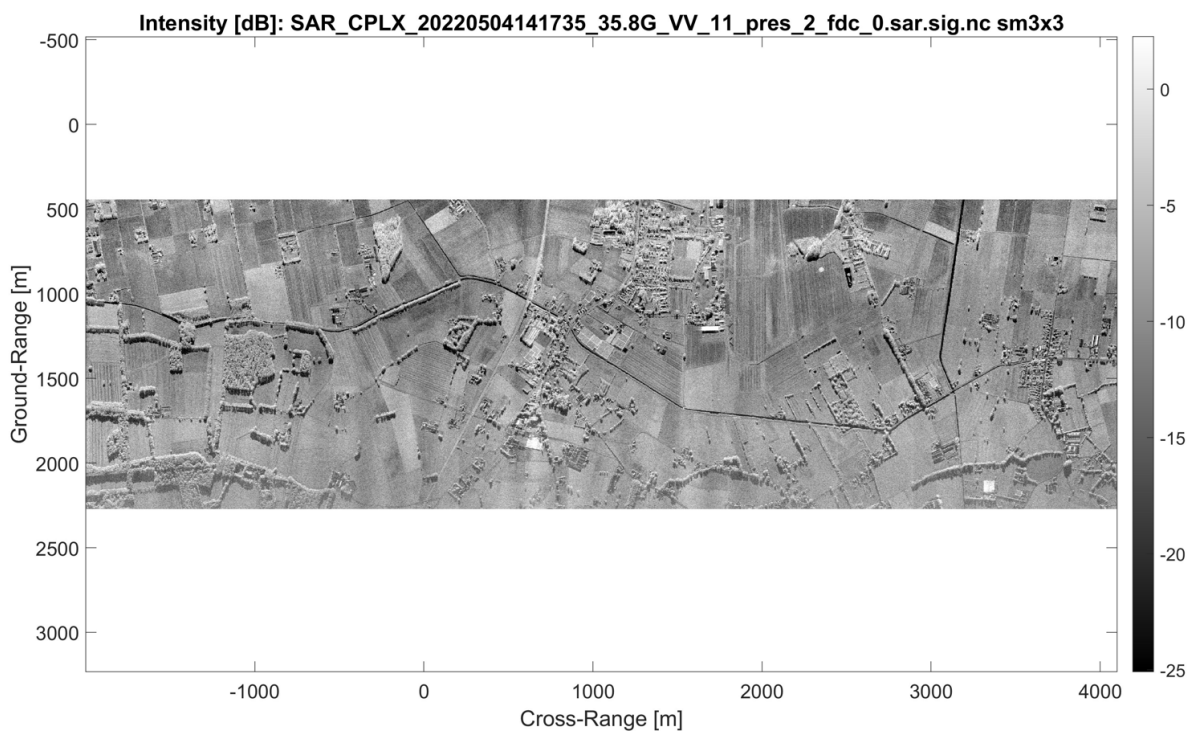


Figure 7: SAR image with swath around 1750 m



Figure 8: NESZ estimation of -25dB.

Figure 9 shows the SAR intensity (3m x 3m) for the full-pol mode acquisition. The RGB composite ((HH is red, VV is blue and HV is green) is presented. A 25 dB of co-pol to cross-pol ratio is verified with the corners. A zoomed-in images shows the expected polarimetric response at the corner's reflector (VV and HH).

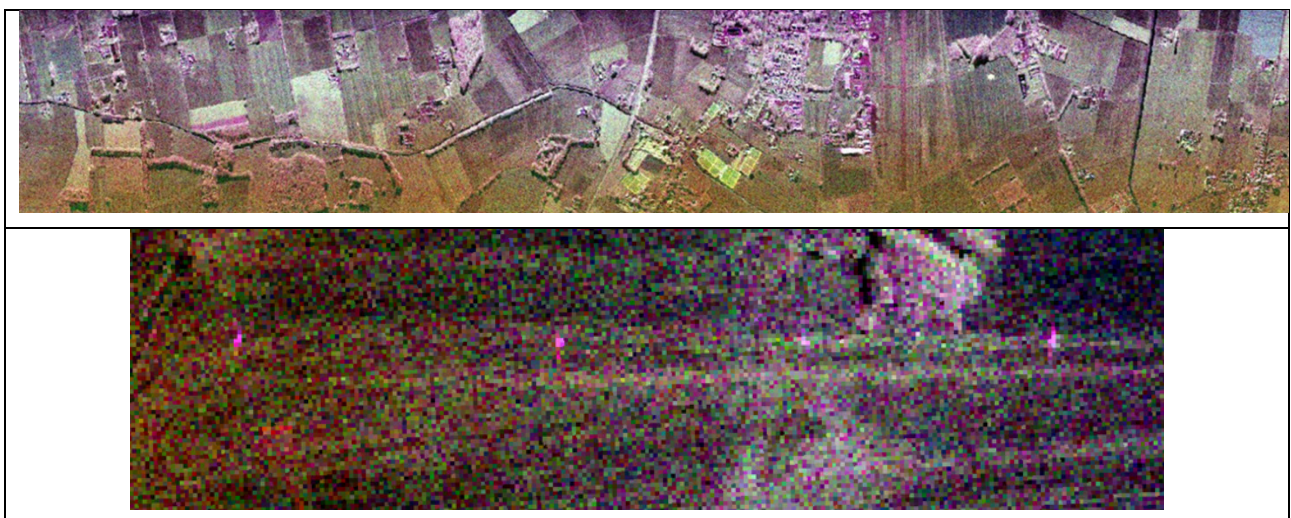


Figure 9: Full-pol KaSAR intensity images [dB] (20220504T163000) from top to bottom: RGB composite ((HH is red, VV is blue and HV is green) and zoomed-in in the corner reflector area.

After the intensity and the radiometry, the interferograms for XTI (Figure 10 upper) and ATI (Figure 10 lower) modes are generated by the KaSAR processor and they show a very accurate interferometric phase.

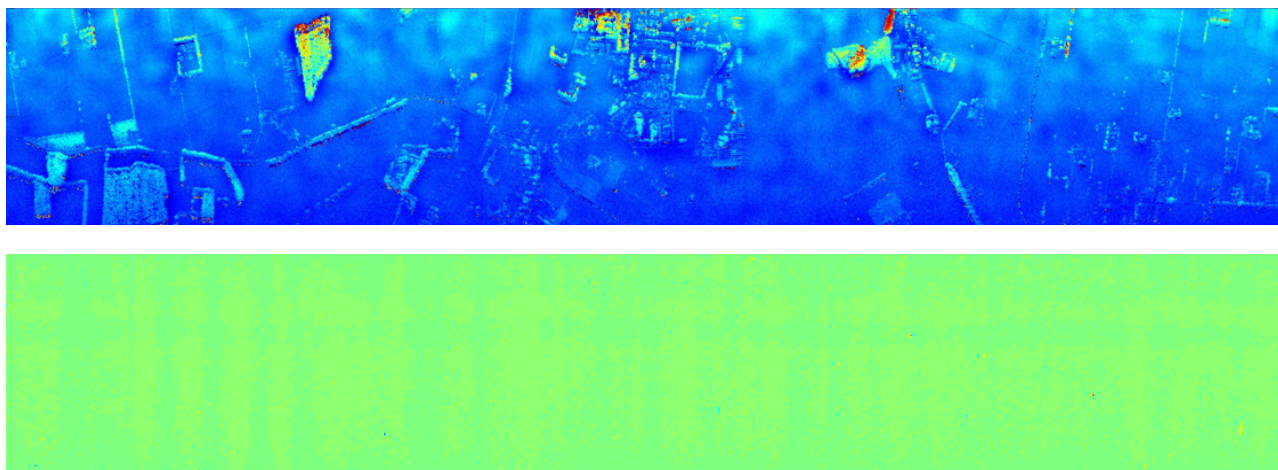


Figure 10: Retrieved Interferograms: XTI above and ATI below

Figure 11 shows the coherence map for the XTI case with very high coherence in the flat terrain and lower when there is vegetation.

Figure 12 shows the Digital Elevation Model retrieved from the above interferograms with a single-pass interferometric SAR.

Figure 13 shows the comparison of height retrieval for the Corner Reflectors in the SAR image (left) and in the DSM (right). On average the error is around 60 cm.

Figure 14 shows the coherence map for the ATI above case with no spatial decorrelation over forest resulting in a very high coherence map.

Figure 15 shows the ATI phases over the corner reflectors for the inter-channel phase accuracy calculation over time.

Figure 16 shows the velocity map over intensity image obtained by KaSAR system. Green is velocity equal zero (steady target) while other colours are moving targets.

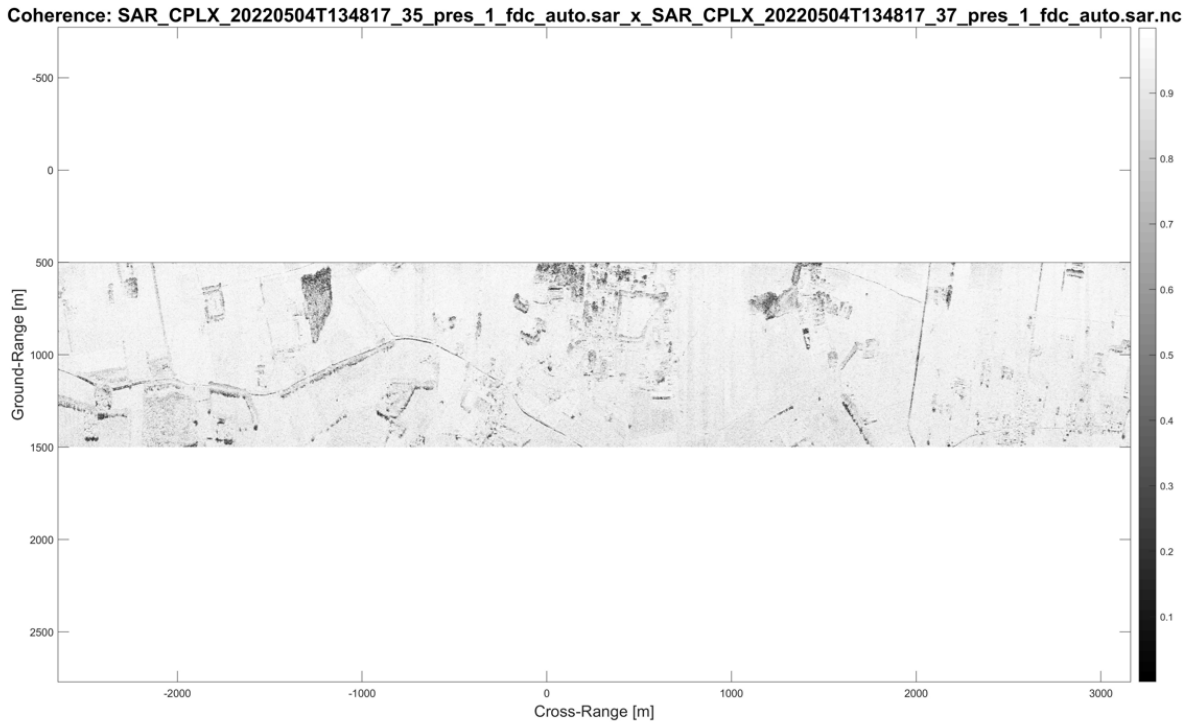
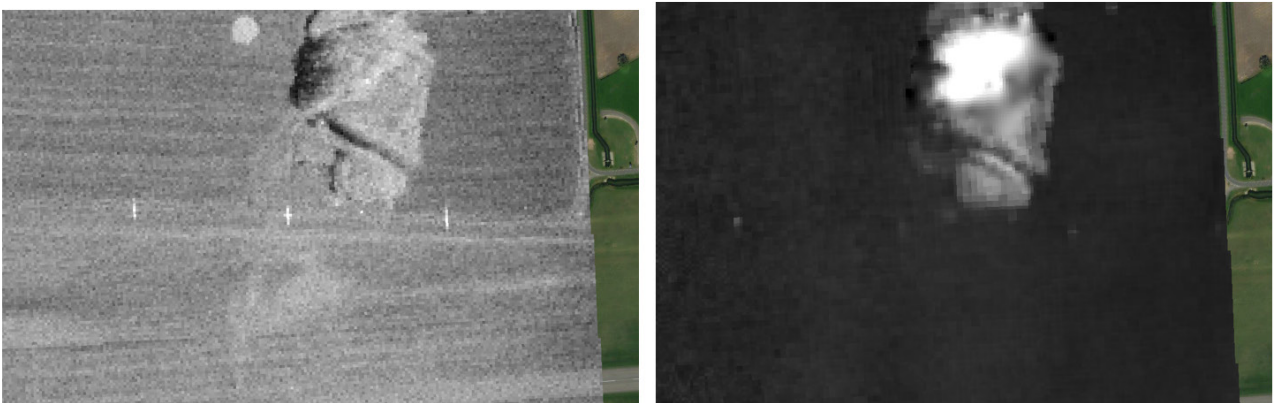


Figure 11: Coherence map for the XTI above case



Figure 12: Digital Elevation Model retrieved from the above interferograms



Corner: C5, C4, C3
 Height = 5.99 m 5.99 m 5.99 m

Corner: C5, C4, C3
 Height = 6.8m 4.4m 5.15m

Figure 13: Comparison of heigh retrieval for the Corner Reflectors. (left - SAR image, right - DSM)

Coherence: SAR_CPLX_20220504T141735_35_pres_1_fdc_auto.sar_x_SAR_CPLX_20220504T141735_39_pres_1_fdc_auto.sar.nc

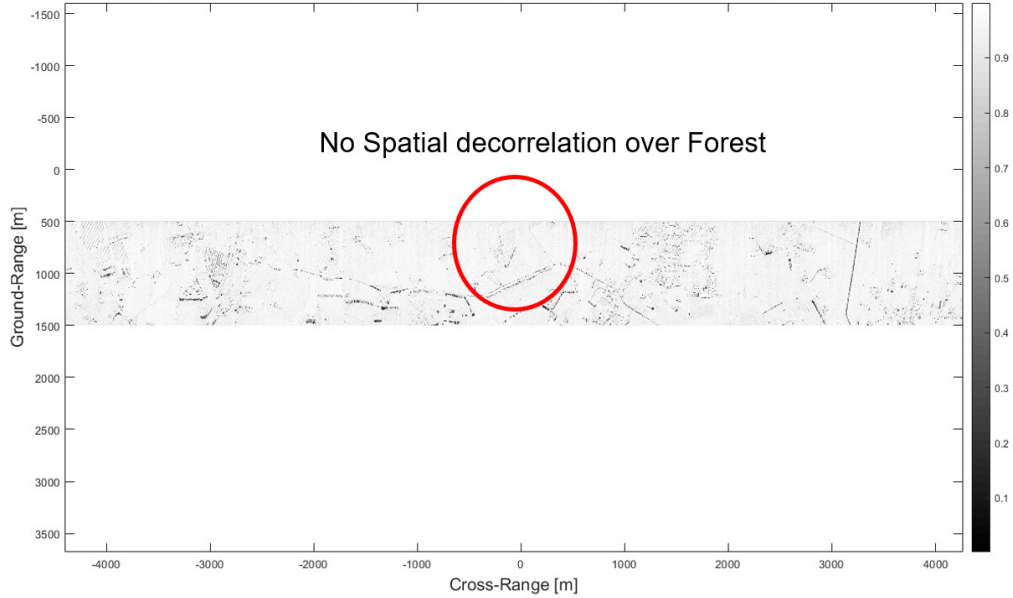


Figure 14: Coherence map for the ATI above case with no spatial decorrelation over forest

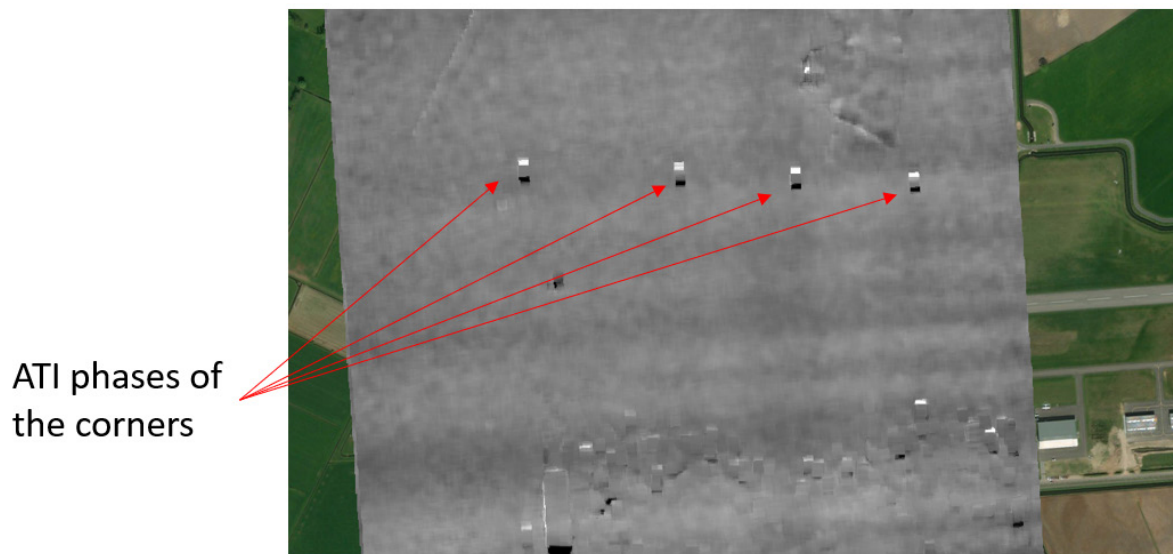


Figure 15: ATI phases of the corners for the inter-channel phase accuracy calculation over time



Figure 16: Velocity map over intensity image.

1.4 Conclusions

The functional verification campaign showed the correct functionalities and operations of the KaSAR system from the data collection with the KaSAR instrument onboard the selected aircraft and the data processing with the KaSAR processor.

The data are correctly collected in different acquisition modes (along-track interferometry, cross-track interferometry, polarimetry), ingested in the pre-processor, and processed to SAR images and interferograms which can be used for further data processing and retrievals.

[END OF DOCUMENT]